Journal of Materials Processing Technology 214 (2014) 1583–1589

Contents lists available at ScienceDirect

Journal of Materials Processing Technology

journal homepage: www.elsevier.com/locate/jmatprotec

Accessing collision welding process window for titanium/copper welds with vaporizing foil actuators and grooved targets

A. Vivek*, B.C. Liu, S.R. Hansen, G.S. Daehn

Department of Materials Science and Engineering, The Ohio State University, 2041 College Road, Columbus, OH 43210, USA

ARTICLE INFO

Article history:
Received 5 September 2013
Received in revised form 27 February 2014
Accepted 1 March 2014
Available online 12 March 2014

Keywords:
Collision welding window
Vaporizing Foil Actuator Welding (VFAW)
Titanium
Copper
Photonic Doppler velocimetry (PDV)
Wavy interface

ABSTRACT

A method for accurate, low-cost, lab-scale determination of the optimal collision angles and velocities for collision welding of a given combination of materials has been introduced. 0.508 mm thick grade 2 CP Ti sheets were launched at various velocities toward a Cu 110 target with grooves of angles ranging from 8° to 28°, machined on the collision side. Capacitor bank-driven aluminum vaporizing foil actuators operated at input energy levels up to 12 kJ and currents up to 140 kA were used to launch the flyer sheets. Velocity was measured with high temporal resolution using a photonic Doppler velocimetry (PDV) system. Collision velocities ranged from 440 m/s to 860 m/s. The welded assemblies were sectioned and the weld interfaces were observed via scanning electron microscopy. For each collision angle there were certain collision velocities which yielded a wavy interface. Welding velocity for transition from smooth to wavy interfaces for each collision angle was used to determine the corresponding transition Reynolds number and was compared to existing results in literature. The uniqueness of this process lies in its small scale and ease of implementation.

© 2014 Elsevier B.V. All rights reserved.

1. Introduction

Collision welding of a given pair of metals occurs only when the collision angles and velocities are within an optimum range, called the welding window. Successful collision welds are generally obtained when the collision velocity is in the range of 150–1500 m/s and the collision angle is between 5° and 20° as cited by Zhang et al. (2011). These ranges can be shown graphically in the form of a welding window. Fig. 1, which is based on the illustration from Akbari Mousavi and Farhadi Sartangi (2009), shows a generic welding window where all the possible outcomes of an attempt for collision welding are presented. Some of the earliest works on welding windows are from Wittman (1973) and Deribas et al. (1975), who studied the effect of explosive welding parameters on the strength and microstructure of welds.

The welding window only indicates the presence or absence of a good weld under a given set of input parameters; it does not quantify the strength of the weld. The shaded area in Fig. 1 denotes the parameters which lead to a wavy interface boundary with no melt zones. In this work, such weld interfaces will be identified and plotted in such graphs. The critical Reynolds number ($R_{transition}$) for laminar to turbulent flow is thought to determine this transition, and is given by the following relation developed by Cowan et al. (1971) who likened wave formation in explosive welding to fluid flow around an obstacle.

$$R_{transition} = \frac{(\rho_{flyer} + \rho_{target})V^2_{F\text{-}transition}}{2(H_{flyer} + H_{target})} = K_{E-P} \quad (1)$$

Here ρ (kg/m^3) stands for density and V_F (m/s) for velocity of flow of the flyer material into the collision point, which approximately equals welding velocity for low collision angles. H represents Vicker's hardness (N/m^2), and K_{E-P} represents the elastic–plastic constant, which varies with collision angle. For low collision angles, it can be shown that V_F and welding velocity (V_W) are almost equal. The relationship between V_W and the collision velocity, V_P, varies with the welding configuration, and will be derived for the present set up. As noted by Crossland (1982), the Karman vortex street analogy should be considered with caution since this is a transient and very local occurrence. This analogy also does not explain why the waves get initiated at a finite distance from the point of first impact. There are other mechanisms that can be considered for wave formation as well: Helmholtz instability, suggested by Hunt (1968), and the interaction of compression and relaxation waves traversing through the colliding plates predicted by Godunov et al. (1970). However, there are inherent problems with those analogies as well. It is possible that for different materials under different conditions,

* Corresponding author. Tel.: +1 6083324892.
E-mail addresses: vivek.4@osu.edu, vivekanupam@gmail.com (A. Vivek).

http://dx.doi.org/10.1016/j.jmatprotec.2014.03.007
0924-0136/© 2014 Elsevier B.V. All rights reserved.

Nomenclature

$R_{transition}$	transition Reynolds number
K_{E-P}	elastic plastic constant
β	collision angle
V_F	velocity of flow of flyer material into the welding front
V_W	welding velocity
V_p	collision velocity
ρ	density (kg/m^3)
H	Vicker's hardness (N/m^2)

one or more of the suggested mechanisms could be at work. The Karman vortex street analogy in conjunction with the Reynolds number is a simple option used by many researchers to mathematically understand the smooth to wavy transition. Due to its simplicity of application, it has been used in this work as well.

Jaramillo et al. (1987) used gas gun-driven experiments to develop the relationship between collision angles and elastic–plastic constants for Al–Al, Cu–Cu and Fe–Fe welds and showed that unlike the theory of Cowan et al., the transition curve is not a straight line but a compromise between Newtonian liquid and elastic–plastic behavior. As shown in the recent simulation work by Grignon et al. (2004) and the experimental work of Akbari Mousavi and Farhadi Sartangi (2009), those relations that depend exclusively on static metallic characteristics of the weld members are still valid. Grignon et al. (2004) also reported some successful finite element modeling work based on Johnson–Cook constitutive model of AA 6061 T0 for modeling the conditions for jetting and smooth-wavy transition criteria during explosive welding. However, a complete model-based solution to this problem, which includes multi-scaled detailed structures, phase transformations at very small levels, and shock physics, has not yet been demonstrated. For the foreseeable future, empirical verification of welding windows created by such numerical or analytical models will be required.

Here, a quick, low-cost method for developing collision welds with varied collision angle and velocity is described. This method can be executed in a typical laboratory. The authors (Vivek et al. (2013) have reported on a novel method for implementing collision welding at length scales similar to magnetic pulse welding (MPW). This method, which has been named Vaporizing Foil Actuator Welding (VFAW), uses the pressure created from electrically driven rapid vaporization of a thin aluminum foil to launch flyer plates of thickness on the order of 1 mm thick to velocities of 1000 m/s or more. The issue of actuator longevity does not exist in this method because the foil actuator is disposable and can be easily replaced after every experiment at a low cost.

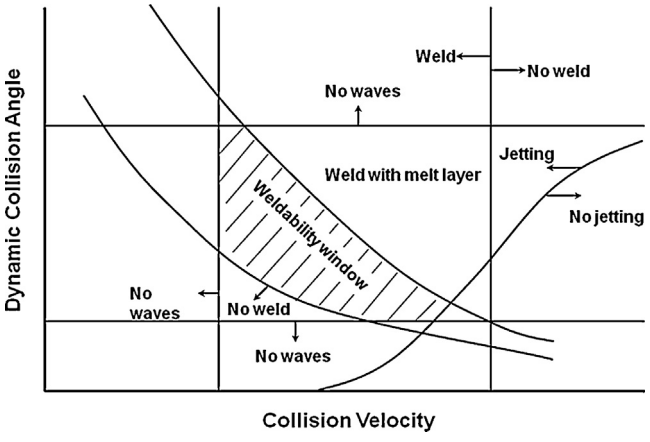

Fig. 1. Generic welding window based on Akbari Mousavi and Satrangi (2009).

Besides explosive, magnetic pulse is also used for high speed flyer launch for collision welding. Daehn (2006) discussed the limitations of both of these methods. Explosive welding (EXW) runs into issues such as the inability to scale the process to thin sheets or small weld zones because explosives do not detonate reproducibly below a certain size known as the critical diameter, which is discussed by Cooper (1997). Furthermore, increasingly stringent safety regulations inhibit their use. The most significant drawback of MPW is that actuators tend to fail after decreasing numbers of cycles as the magnetic pressure increases. Laser-driven collision welding (Zhang et al., 2011) also has a niche, but because the delivered energies are typically on the order of several joules, this is not suitable for workpieces on the size scale of centimeters. Filling this gap has also been a motivation for developing VFAW.

The work presented here focuses on using VFAW for determination of the welding window of commercially pure titanium and copper. Following a brief description of the experimental procedure, the results are discussed and plotted on charts resembling welding windows from Jaramillo et al. (1987) and Akbari Mousavi and Farhadi Sartangi (2009). An empirical relation between K_{E-P} and β is also derived.

2. Experimental procedure

The Vicker's hardnesses of the copper and titanium to be welded were measured to be 90 HV and 170 HV, respectively. Specific angles (8°, 12°, 16°, 20°, 24°, and 28°) were machined into a 6.3-mm-thick copper target plate in the form of grooves. These angled grooves provide the collision angles required for collision welding. A piece of dogbone-shaped 0.0762-mm-thick aluminum foil was connected to the leads of a 426-μF capacitor bank, the characteristics of which are cited in Table 1.

The 0.5-mm-thick titanium flyer was placed against the foil actuator, with polyester and polyimide insulation in between, using procedures similar to those described by Vivek et al. (2013). The copper target plate with the angled grooves was placed parallel to the flyer, with a 1.6-mm stand-off gap in between. The whole assembly was clamped in a fixture made of heavy steel blocks. Fig. 2 shows different stages and views of the experimental assembly. The capacitor bank was charged to various energy levels (3, 4, 6, 8, 10, and 12 kJ) and then rapidly discharged through the foil. The foil was effectively and instantly vaporized by the high current and generated sufficient pressure to propel the flyer into a high-speed collision with the target plate. The experiment was repeated one extra time at 8 kJ to test reproducibility. The velocity of the flyer was measured in situ at each energy level by a photonic Doppler velocimetry (PDV) system (Johnson et al., 2009). The PDV probe looked at the flyer plate through concentric holes that were drilled in the steel backing block and the copper target plate to measure the normal sheet velocity, V_P. If the angle of collision is β, then from Fig. 3 it can be geometrically shown that

$$V_W = \frac{V_P}{\sin(\beta)} \approx V_F \quad (2)$$

The approximate equality between V_W and V_F holds true as long as β is small (<30°). Voltage was measured using a 1000:1 probe connected across the terminals of the capacitor bank, and current was measured by a 100kA:1 V Rogowski coil. The samples were then sectioned for metallography and mechanical testing.

Table 1
Capacitor bank characteristics.

Capacitance	Inductance	Resistance	Maximum charging voltage	Maximum charging energy	Short circuit current rise time
426 μF	100 nH	10 mΩ	8.66 kV	16 kJ	12 μs

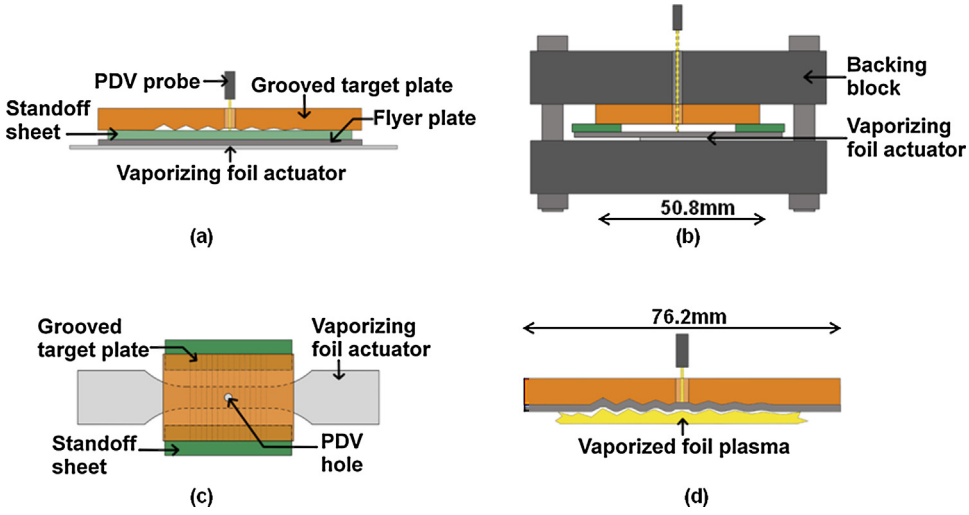

Fig. 2. Experimental set up for the welding window determination using VFAW: (a) side view showing the angled grooves in the target plate, (b) front view showing the positioning of the standoffs, (c) top view, (d) mid-experiment side view of the weld interface.

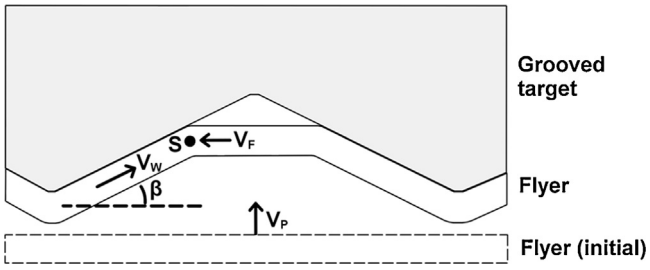

Fig. 3. A schematic representation of the progress of welding process. S is the collision point which moves at a velocity V_w as the weld progresses.

3. Results and discussion

Flyer launch at different input energy levels led to the velocity-displacement histories shown in Fig. 4. With the exception of the 12 kJ shot, which in a separate experiment was found to be anomalous, the flyer velocity increased with increasing input energy. Collision velocity decreased from 860 m/s for 10 kJ to 800 m/s for the 12 kJ experiment. Nevertheless, the data obtained at 12 kJ input energy was still usable as the flyer velocity, not its relation with input energy, is of interest for this work. Also, the velocity curves for the two 8 kJ experiments overlaid very closely. Since the initial standoff was 1.6 mm, the collision velocities were measured at that distance and are shown in Table 2.

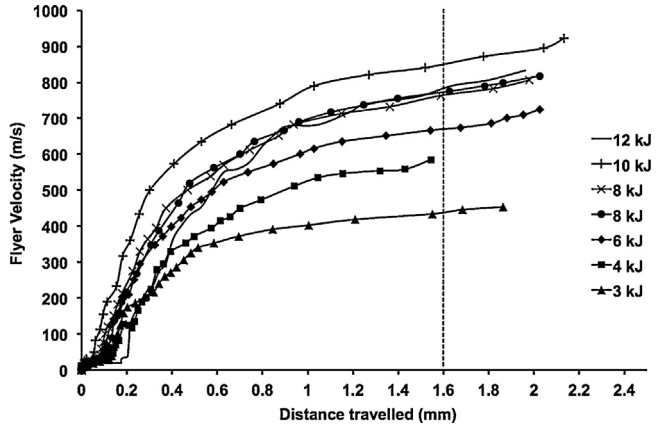

Fig. 4. Flyers' velocity evolution with respect to distance traveled due to its launch by vaporizing foil actuator at different input energies.

Three types of weld interfaces as shown in Fig. 5 were obtained during this run of experiments. Here, V_W was calculated based on collision velocity (V_P) and β from Eq. (2). If the velocity was too high for a given collision angle then melting along the interface was observed, while if it was too low then very weak or no welds were formed. If the welding velocity and collision angles were within the welding window then a wavy interface with no melt zones was observed. Figs. 6 and 7 show the weld interfaces obtained due to flyer impact into grooves of different angles. The interfaces obtained by the other experiment done with an 8 kJ input energy are also shown in Fig. 7, and the results were found to be reproducible.

The samples generated from this run of experiments do not lend well to peel testing since they have V-shaped grooves. However, a comparative test was implemented for the welds created at different collision velocities with the grooves of the same angle. The same peel testing apparatus as used by Vivek et al. (2013) was used for these tests. Although this peel test needs to be improved and standardized, it gives a good indication about the strength of the welds. According to Figs. 6 and 7, a 12° collision angle demonstrated a transition from smooth to wavy interface followed by a transition back to smooth interface with melting. Peel test samples were prepared for collision velocities of 440 m/s, 670 m/s, 770 m/s, and 860 m/s. The 440 m/s sample came apart during sample

Table 2
Collision velocity for different input energy levels.

Input electrical energy (kJ)	3	4	6	8	8	10	12
Collision velocity (m/s)	440	585	670	770	767	860	800

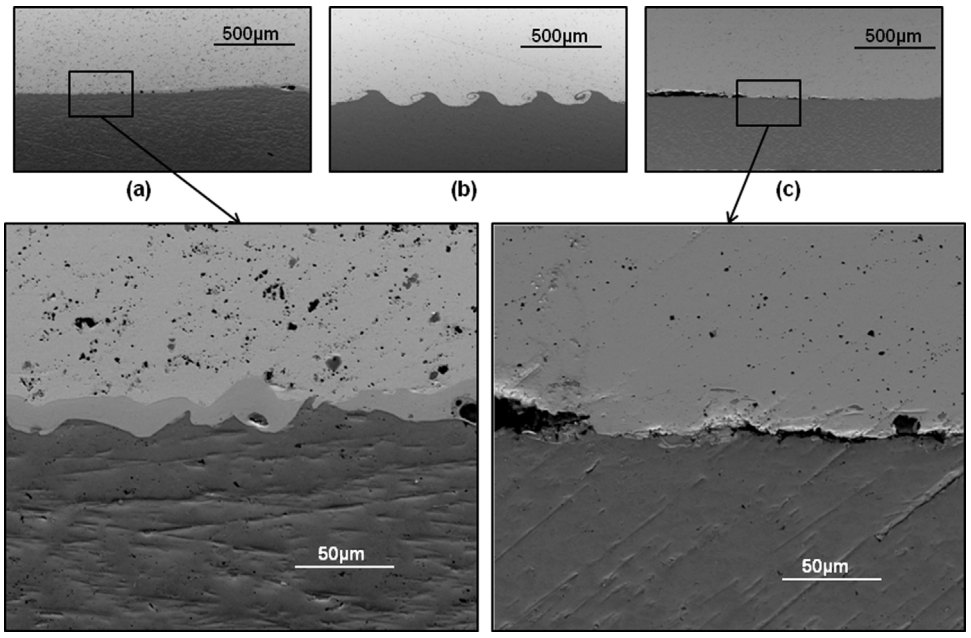

Fig. 5. Three different types of weld interfaces: (a) melted due to excessive V_W (5748 m/s) for a given β (8°), (b) wavy for ideal V_W (1893 m/s) for a given β (24°), (c) un-welded due to insufficient V_W (937 m/s) for a given β (28°).

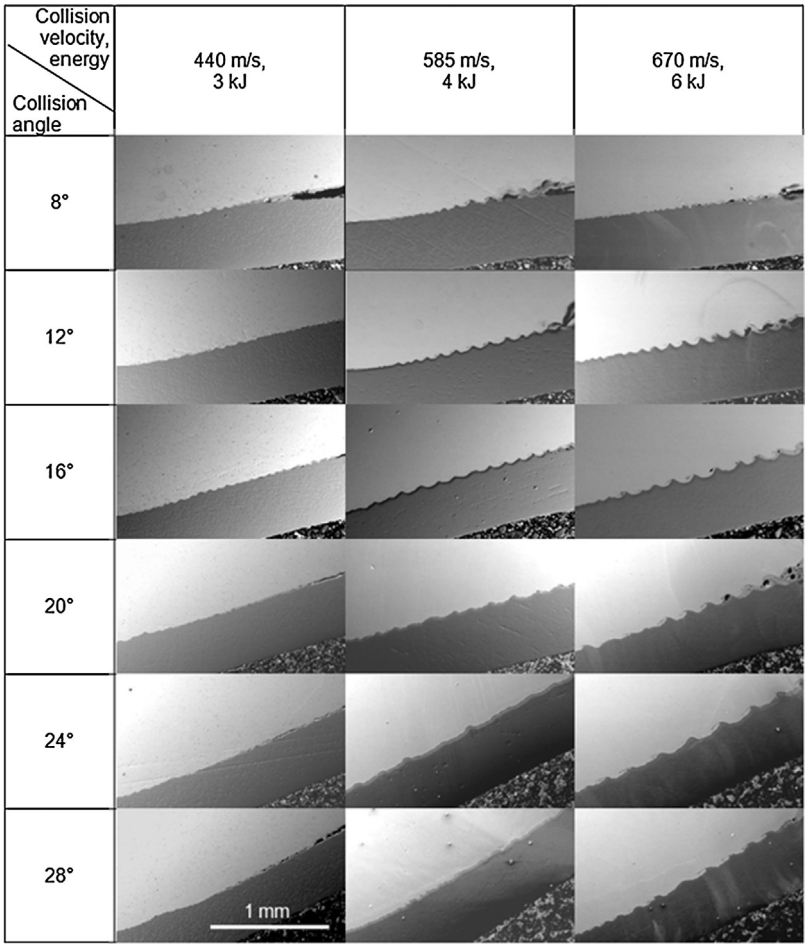

Fig. 6. SEM images showing the wavy or smooth interfaces of the welds created at different collision angles, with collision velocities between 440 m/s and 670 m/s.

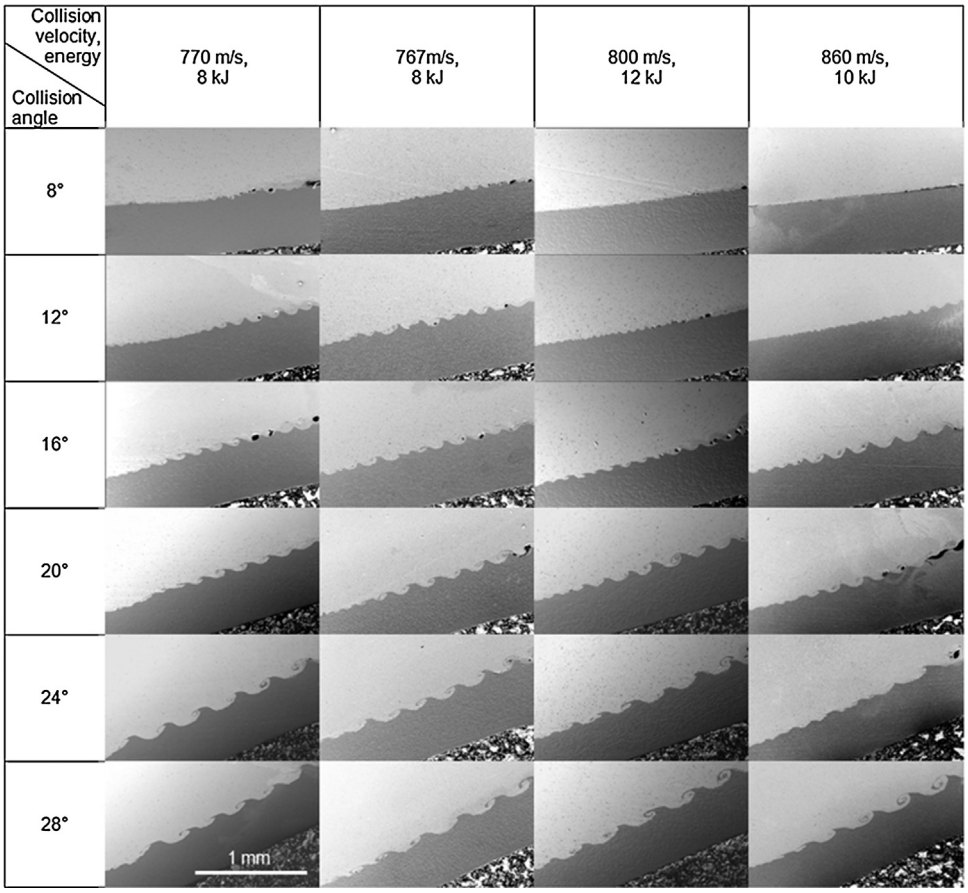

Fig. 7. SEM images showing the wavy or smooth interfaces of the welds created at different collision angles, with collision velocities between 767 m/s and 860 m/s.

preparation since the weld interface was either very weak or non-existent. The force-displacement data for the other three samples are shown in Fig. 8. The peak force was the highest for the wavy interface welds. More importantly, fracture occurred along the interface in case of the melted interface, whereas, the laminate broke in the parent titanium sheet in the case of the wavy interfaces. Further experimentation with different material combinations would be required to completely justify the hypothesis that wavy interface always corresponds to the strongest welds.

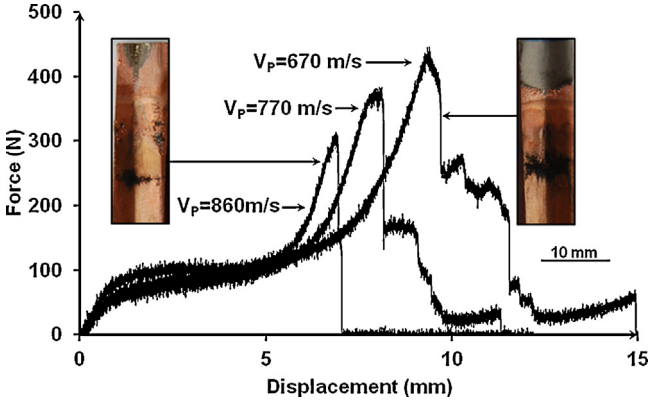

Fig. 8. Force vs displacement data for peel testing of welds created at 12° collision angle and different collision velocities. Different zones of failure in the representative peel test specimens inset in the figure should be noted. The weld created at V_P = 860 m/s had a smooth interface and failed along the interface, whereas, the one created at V_P = 670 m/s had a wavy interface and failed in parent titanium sheet.

The cases where a wavy interface was obtained are noted in Fig. 9. The data set fits into the windows which are shaped similar to the ones obtained by Deribas et al. (1975) and Jaramillo et al. (1987), as shown in Fig. 9. It is interesting that waves were observed for low collision velocities along the 8° groove's interface, which became smooth for collision velocities greater than 600 m/s. Localized melting was also observed along that interface at high velocities. Therefore, higher velocity may not necessarily result in a good weld. It is also interesting to note that higher collision angles also may not necessarily result in a wavy interface. This is evidenced by the transition from wavy to smooth for a collision velocity of 585 m/s when the collision angle changes from 16° to 20°. All of these results are also summarized in Fig. 9.

The data in Fig. 10(a) can be used to determine the relation between the elastic–plastic constant for copper-titanium pair. The lowest welding velocity required for transition from a smooth to a wavy interface for each collision angle was first used to calculate the corresponding Reynolds number.

Fitting a cubic polynomial through the K_{E-P} vs. collision angle plot in Fig. 10(b) resulted in the following relation:

$$K_{E-P} = 175.53 - 15.995\beta + 0.5174\beta^2 - 0.0053\beta^3, \quad \text{correlation} = 0.9174 \tag{3}$$

The equations derived by Jaramillo et al. were for similar material couples which could explain why they are different than the one derived here in terms of the constant and the coefficients. The K_{E-P} values estimated here for corresponding collision angles are almost 4 times larger than those obtained by Jaramillo et al. (1987). This means that smooth to wavy transition happened at twice the

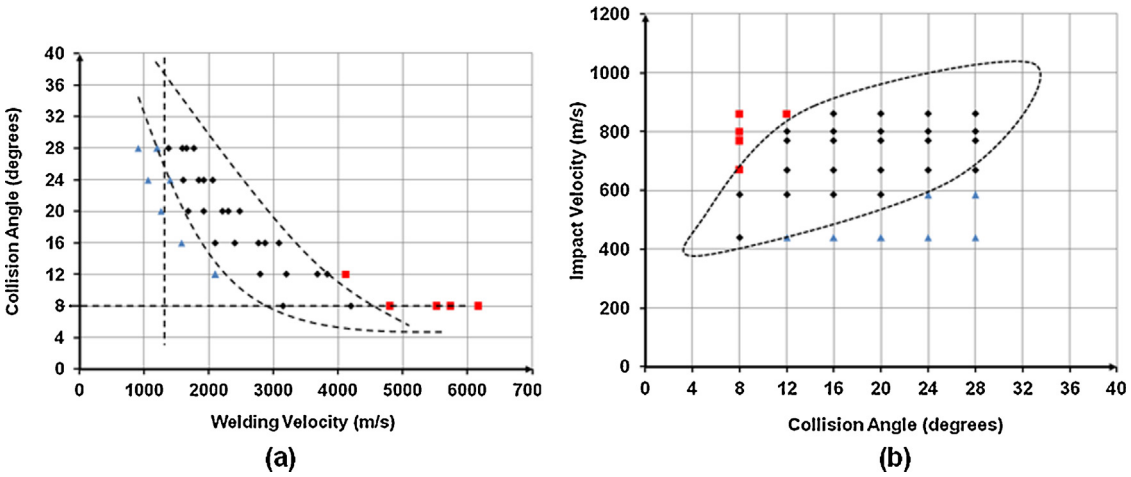

Fig. 9. Welds with different types of interfaces: (a) collision angle vs. welding velocity shown in a window proposed by Deribas et al. (1975), (b) collision velocity vs. collision angle fitted inside a window proposed by Jaramillo et al. (1987). ♦ = wavy interface with no melt layer, ■ = melt layer at the interface, ▲ = voids and cracks at interface.

velocity relative to their work. It was also reported by Jaramillo et al. (1987) that thinner flyer plates can lead to higher transition velocities and subsequently higher K_{E-P}, which was definitely the case here for the flyer plates which are about 0.5 mm thick.

Since this is an ongoing work, the data chart presented in Fig. 10 could be incomplete, and more experiments would need to be done to gain more confidence in the derived Eq. (3). Although the results of the two 8 kJ experiments shown here were very similar, further characterization of repeatability of this method should be done. The welds obtained here are with collision velocities at an interval of nearly 100 m/s. It is possible that there are some transitions that were missed due to large intervals in collision velocity data. The transition welding velocity assumed for 8° groove may not be the real transition velocity as it was simply the lowest velocities obtained. There are also a few other assumptions that were made during this process. For example, the velocity measured at the center of the flyer was considered to be representative of the velocities everywhere on the flyer. This is a reasonable assumption since the foil actuator was designed to ensure a homogenous burst upon passage of current; hence pressure on the flyer can also be assumed to be uniform. In a separate experiment, the velocities of two points on the flyer, 15 mm apart, were different by 20 m/s. Additionally, since the distance traveled by the flyer is quite small and it is constantly driven by the formed gases, the collision velocity and angle are assumed to stay constant as the flyer collapses onto the grooved target.

Further analysis similar to the work done by Grignon et al. to calculate other welding window parameters can be done using the data obtained in this work. It has been shown that this process can be used to obtain similar data and perform similar analysis to that which has been traditionally done through explosives and gas guns. This technique also offers a tool for understanding the effect of flyer sheet thickness on smooth-wavy transition criteria and the size of the waves. These effects of target thickness variation have been studied earlier by Ben-Artzy et al. (2010) with regard to wave formation mechanisms based on wave theory, and can be verified using VFAW in a future study. According to Göbel et al. (2012), the welding windows of EXW and MPW are not necessarily the same. Perturbations in the path of the flyer can also cause wave initiation along the interface. Due to much smaller length scales of MPW as compared to EXW, a metastable wave initiation mechanism was reasoned to be the cause for smooth to wavy transition at lower welding front velocity during MPW. The size scales implemented with VFAW are similar to those of MPW and the velocities achievable are in the regime of EXW. A multi-scale study would be required to fully determine the interchangeability of process windows developed from this tool to other welding techniques.

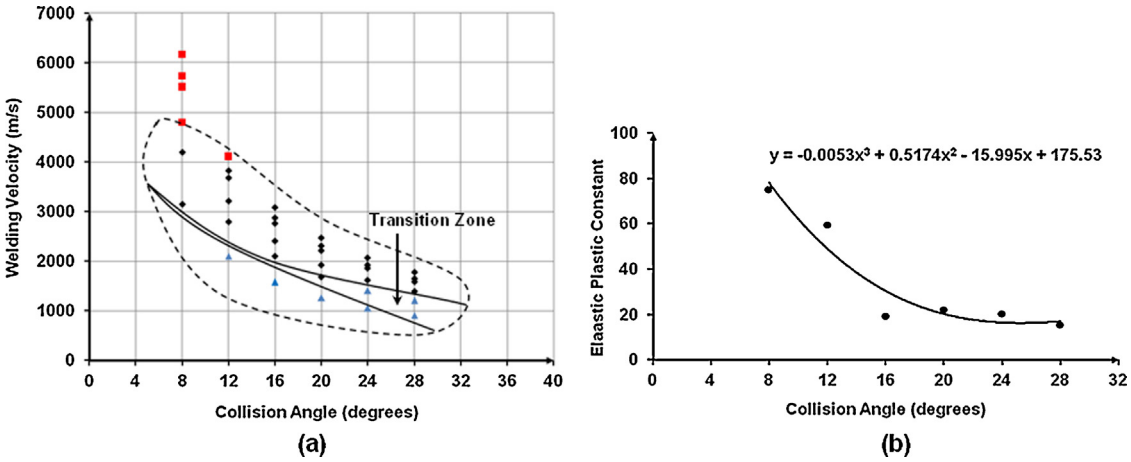

Fig. 10. Welds with different types of interfaces. (a) welding velocity vs. collision angle data fitted inside a window conceptualized by Jaramillo et al. (1987), (b) derived elastic–plastic constant for transition from smooth to wavy interface at different collision angles. ♦ = wavy interface with no melt layer, ■ = melt layer at the interface, ▲ = voids and cracks at interface.

4. Final remarks and conclusions

Based on the work, following remarks and conclusions can be made:

(1) VFAW was used for the first time for welding window determination of CP Ti–Cu couple. A relation between the elastic–plastic constant and collision angle was developed for this pair of materials. The fitted curve was higher than the one obtained in earlier works with similar metal pairs. Small flyer plate thickness could be a reason for the difference.
(2) Low angle at high velocities led to smooth interfaces with a melt layer. Given sufficient welding velocities, melt layers can occur at higher angles as well, but such conditions were not reached in this work.
(3) VFAW serves as a small-scale, low-cost, and repeatable method for welding window determination. Further experimentation needs to be conducted to increase the number of data points and establish a more statistically reliable model. Although a large range of velocities (440–860 m/s) were investigated, this range needs to be expanded further in order to populate the welding window chart fully.

Acknowledgements

The authors would like to thank the Alcoa Foundation, which supported the work through the Advancing Sustainability Research Initiative.

References

Akbari Mousavi, S.A.A., Farhadi Sartangi, P., 2009. Experimental investigation of explosive welding of cp-titanium/AISI 304 stainless steel. Materials & Design 30 (3), 459–468.
Ben-Artzy, A., Stern, A., Frage, N., Shribman, V., Sadot, O., 2010. Wave formation mechanism in magnetic pulse welding. International Journal of Impact Engineering 37 (4), 397–404.
Cooper, P., 1997. Real effects in explosives. Explosives Engineering, 290–293.
Cowan, G.R., Bergmann, O.R., Holtzman, A.H., 1971. Mechanism of bond zone wave formation in explosion-clad metals. Metallurgical and Materials Transactions B 2 (11), 3145–3155.
Crossland, B., 1982. Explosive Welding of Metals and its Application. Clarendon Press, Oxford, pp. 26–29.
Daehn, G.S., 2006. High-velocity metal forming. In: Metalworking: Sheet Forming. ASM Handbook, vol. 14B. ASM International, pp. 405–418.
Deribas, A.A., Simonov, V.A., Zakcharenko, I.D., 1975. Investigations on explosive welding parameters for arbitrary combinations of metals and alloys. Sixth International Conference on High Energy Rate Fabrication 4 (1), 1024.
Göbel, G., Beyer, E., Brenner, B., Kaspar, J., 2012. Dissimilar metal joining: macro- and microscopic effects of MPW. In: 5th International Conference on High Speed Forming, pp. 170–188.
Godunov, S.K., Deribas, A.A., Zabrodin, A.V., Kozin, N.S., 1970. Hydrodynamic effects in colliding solids. Journal of Computational Physics 5 (3), 517–539.
Grignon, F., Benson, D., Vecchio, K.S., Meyers, M.A., 2004. Explosive welding of aluminum to aluminum: analysis, computations and experiments. International Journal of Impact Engineering 30 (10), 1333–1351.
Hunt, J.N., 1968. Wave formation in explosive welding. Philosophical Magazine 17 (148), 669–680.
Jaramillo, D., Szecket, A., Inal, O.T., 1987. On the transition from a waveless to a wavy interface in explosive welding. Materials Science and Engineering 91, 217–222.
Johnson, J.R., Taber, G., Vivek, A., Zhang, Y., Golowin, S., Banik, K., Fenton, G.K., Daehn, G.S., 2009. Coupling experiment and simulation in electromagnetic forming using photon Doppler velocimetry. Steel Research International 80 (5), 359–365.
Vivek, A., Hansen, S.H., Liu, B.C., Daehn, G.S., 2013. Vaporizing foil actuator: a tool for collision welding. The Journal of Materials Processing Technology 213 (12), 2304–3231.
Wittman, R.H., 1973. The influence of collision parameters on the strength and microstructure of an explosion welded aluminum alloy. In: Proceedings of 2nd Symposiun on Use of Explosive Energy in Manufacturing Metallic Materials of New Properties and Possibilities of Application thereof in the Chemical Industry, pp. 153–168.
Zhang, Y., Babu, S.S., Prothe, C., Blakely, M., Kwasegroch, J., LaHa, M., Daehn, G.S., 2011. Application of high velocity impact welding at varied different length scales. Journal of Materials Processing Technology 211 (5), 944–952.